AAC Journals.ASM.org

Toxicity Mechanisms of Amphotericin B and Its Neutralization by Conjugation with Arabinogalactan

Sarah Kagan,[a] Diana Ickowicz,[b] Miriam Shmuel,[b] Yoram Altschuler,[b] Edward Sionov,[a]* Miriam Pitusi,[a] Aryeh Weiss,[c] Shimon Farber,[b] Abraham J. Domb,[b] and Itzhack Polacheck[a]

Department of Clinical Microbiology and Infectious Diseases, Hadassah-Hebrew University Medical Center, Jerusalem, Israel[a]; The Institute for Drug Research, School of Pharmacy, The Hebrew University of Jerusalem, Jerusalem, Israel[b]; and Bio-Imaging Unit, Silverman Institute of Life Sciences, The Hebrew University of Jerusalem, Jerusalem, Israel[c]

Amphotericin B (AMB) is an effective antifungal agent. However, its therapeutic use is hampered by its toxicity, mainly due to channel formation across kidney cell membranes and the disruption of postendocytic trafficking. We previously described a safe injectable AMB-arabinogalactan (AG) conjugate with neutralized toxicity. Here we studied the mechanism of the toxicity of free AMB and its neutralization by conjugation with AG. AMB treatment of a kidney cell line modulated the trafficking of three receptors (C-X-C chemokine receptor type 4 [CXCR4], M1 receptor, and human transferrin receptor [hTfnR]) due to an increase in endosomal pH. Similar data were also obtained in yeast but with an increase in vacuolar pH and the perturbation of Hxt2-green fluorescent protein (GFP) trafficking. The conjugation of AMB with AG neutralized all elements of the toxic activity of AMB in mammalian but not in fungal cells. Based on these results, we provide an explanation of how the conjugation of AMB with AG neutralizes its toxicity in mammalian cells and add to the knowledge of the mechanism of action of free AMB in both fungal and mammalian cells.

Opportunistic fungal infections have emerged as an important cause of morbidity and mortality in immunodeficient patients (34). Amphotericin B (AMB) is considered one of the most effective antifungal agents; it exhibits wide-spectrum activity against both filamentous and yeast-like fungi, its pharmacokinetic and pharmacodynamic profiles are superior to those of other antifungal agents, and it is fungicidal, in contrast to most azoles which are fungistatic (3, 39, 53). The fungicidal effect is important, since most patients suffering from invasive fungal infections are immunocompromised (34). However, the infusion-related and cumulative toxicities, particularly nephrotoxicity (14, 20, 30), of AMB have resulted in reductions in the routine use of deoxycholate micellar AMB formulations and the development of less-toxic high-cost lipid AMB formulations (16, 36). To develop a soluble, less-toxic, and less costly formulation, AMB has been conjugated with various soluble macromolecules (18, 37, 47–49).

We conjugated AMB with arabinogalactan (AG) (18), which significantly increased the water solubility of AMB, reduced its toxicity, and resulted in an efficacy similar to that of Fungizone (a deoxycholate micellar formulation) and AmBisome (a lipid-based formulation) (18). AMB-related toxicity is associated with the inductions of interleukin 1β (IL-1β), tumor necrosis factor α (TNF-α), and apoptosis in organs. These effects were not observed with the AMB-AG conjugate (AMB-AGC), suggesting its potential as a safer formulation for therapeutic use (19). AG is an inexpensive natural product, and the conjugation reactions are performed at room temperature, revealing promise for a potentially low-cost drug. AMB penetrates the plasma membrane (PM) and interacts with its sterols to form transmembrane channels, resulting in the leakage of monovalent ions and metabolites, which leads to cell death (5, 22, 45). The therapeutic use of AMB as an antifungal agent is based on its higher affinity to ergosterol, the main sterol in fungal membranes, than to cholesterol. In addition, AMB generates a larger and more stable pore in ergosterol-containing membranes than in their cholesterol-containing counterparts in mammalian cells (4, 12). AMB channel assembly in cholesterol-containing membranes requires the formation of AMB dimers or oligomers in the surrounding media, whereas AMB monomers are sufficient for channel assembly in ergosterol-containing membranes (6, 7, 25, 26, 31, 32), suggesting that AMB monomers are responsible for the antifungal selectivity.

Following the treatment of CHO (Chinese hamster ovary) cells with AMB, Vertut-Doi et al. (56) showed that the drug is endocytosed and transported to the lysosomal compartment. AMB at high concentrations (50 μM) accumulated in the PM and in the endosomes but not in the lysosomes. This localization indicated inhibition of intracellular traffic from endosomes to lysosomes. An additional effect of AMB on endocytosis and postendocytic trafficking was observed with sulforhodamine B, a fluid-phase marker of endocytosis (56). AMB treatment of MDCK cells (Madin-Darby canine kidney epithelial cell line) resulted in the loss of surface caveolae, the redistribution of caveolin-1 and caveolin-3 from the PM to large internal ring-shaped structures identified as enlarged early and late endosomes, and the relocalization of caveolar proteins from the PM to the caveolin-positive endosomes (10).

This broad effect on membrane trafficking might be another

Received 19 March 2012 Returned for modification 28 May 2012
Accepted 7 August 2012
Published ahead of print 20 August 2012
Address correspondence to Itzhack Polacheck, itzhackp@ekmd.huji.ac.il.
* Present address: Edward Sionov, Laboratory of Clinical Infectious Diseases, National Institutes of Health, Bethesda, Maryland, USA.
Supplemental material for this article may be found at http://aac.asm.org/.

doi:10.1128/AAC.00612-12

mechanism governing AMB activity. In addition, disruption of the pH gradient between endosomes and the cytosol has been shown to stop numerous intracellular trafficking pathways in mammalian cells (15, 21, 27, 33, 42). An association between intraendosomal pH and trafficking has also been found in yeast (1). In *Candida albicans* labeled with the fluorescent pH indicator BCECF [2′,7′-bis-(2-carboxyethyl)-5-(and-6)-carboxyfluorescein acetoxymethyl ester], AMB treatment induced an increase in fluorescence intensity, indicating an increase in vacuolar pH (59). Hence, we hypothesized that AMB exerts its effects on trafficking through endosomal perforation and alkalization; therefore, the goal of this study was to investigate the effects of AMB and AMB-AGC treatment on membrane integrity, intracellular trafficking, and endosomal/vacuolar pH in both epithelial and yeast cells.

MATERIALS AND METHODS

AMB-AGC synthesis. AMB-AGC was synthesized by the conjugation of AMB (Alpharma, Copenhagen, Denmark) with oxidized AG as described previously (17, 18).

Growth conditions. The *Candida albicans* strain ATCC 90028 (American Type Culture Collection, Manassas, VA) and the *Saccharomyces cerevisiae* CRY1 strain W303 expressing the hexose transporter 2 (Hxt2)-green fluorescent protein (GFP) construct (57) were grown for 48 h at 35°C on Sabouraud dextrose agar (SDA plates; Novamed, Jerusalem, Israel). Vero and MDCK-PTR9 cells (9) were grown in an incubator (37°C, 5% CO_2) in Dulbecco's modified Eagle medium (DMEM) (containing 10% fetal calf serum [FCS], 10 mM HEPES, 1% penicillin-streptomycin solution) and minimum essential medium Eagle (MEM-EAGLE) (containing 5% FCS, 1% penicillin-streptomycin solution), respectively (all media and related reagents were purchased from Biological Industries, Beit Haemek, Israel).

Antifungal susceptibility testing. The MIC values were determined according to CLSI recommendations (11).

AMB and AMB-AGC killing curves for *C. albicans*. Exponential-phase yeast cells (5×10^6 cells/ml) were incubated in 2% glucose-yeast extract-peptone-dextrose (YPD) broth with AMB/AMB-AGC at 37°C. At the appropriate time points, samples after serial dilutions were plated in triplicate on RPMI 1640 medium (Novamed).

K^+ leakage test in *C. albicans*. K^+ leakage was determined by atomic absorption spectroscopy as described previously (41).

***C. albicans* vacuolar pH measurement.** *C. albicans* (grown overnight at 30°C in RPMI medium) was labeled with the fluorescent intracellular pH indicator BCECF-AM (Biotum, Inc., Hayward, CA) (59), and 150 μl of a 2×10^6 cell/ml suspension was incubated at room temperature (RT) in black 96-well Nunc plates with AMB/AMB-AGC at various concentrations. The plates were read in a Tecan SpectraFluor Plus multi-well plate reader (excitation, 450 and 492 nm; emission, 535 nm). A calibration curve was prepared with free BCECF (Biotum, Inc.) (13).

SRBC hemolysis. The hemolytic effect of AMB/AMB-AGC on sheep red blood cells (SRBCs) was studied as described previously (17).

AMB and AMB-AGC effects on Vero- and MDCK-cell viability. Cell viabilities were determined after the incubation of cells (1.6×10^5 cell/ml) with various concentrations of AMB/AMB-AGC in a 96-microwell plate at 37°C in 5% CO_2 for 1 h and 19 h for Vero and MDCK-PTR9 cells, respectively. Viabilities were tested with the 2,3-bis(2-methoxy-4-nitro-5-sulfophenyl)2H-tetrazolium-5-carboxanilide (XTT)-based cell-proliferation kit (Biological Industries). The plates were read at 450 nm in a microwell system reader (Organon Technica, Oss, Netherlands).

K^+ leakage test in Vero cells. Vero cells (in 10-cm plates) were incubated for 1 h with AMB/AMB-AGC, washed with saline, and disrupted by incubation (70°C, 1 h) with 5 ml distilled deionized water (DDW). The supernatant K^+ concentration was determined by a Perkin Elmer 403 atomic absorption spectrophotometer (Perkin Elmer Corp., Norwalk, CT) at 383 nm, calculated according to a KCl calibration curve, and normalized to the number of cells.

Hxt2-GFP endocytosis assay. The exponential-phase culture of *S. cerevisiae* in 5% glucose-YPD broth (37°C, 18 h, 150 rpm) was transferred after washing to 0.2% glucose-YPD for 4 h and then back to 5% glucose-YPD with or without AMB/AMB-AGC. After a 70-min incubation, the cells were fixed with 4% paraformaldehyde/3.4% sucrose, preserved in a KPO_4/sorbitol solution (1.2 M sorbitol, 0.1 M potassium phosphate [pH 7.5]), and analyzed by fluorescence microscopy.

M1-GFP localization. The MDCK cells stably expressing the M1-GFP construct (51) were grown on glass coverslips, treated with AMB/AMB-AGC (1 h), and fixed with 4% paraformaldehyde (2). Images were captured using a Nikon TE-2000S inverted-fluorescence microscope (Nikon, Melville, NY) with a plan Apo 60× objective lens and processed with Image-Pro Plus v4.5 software (Media Cybernetics, Inc., Bethesda, MD).

MDCK cell internalization of human transferrin. MDCK-PTR9 cells were grown for 2 days on glass coverslips followed by overnight or 24-h transferrin starvation in MEM/bovine serum albumin (BSA) medium (MEM Hanks' balanced salts [GIBCO, Grand Island, NY] containing 25 mM HEPES [pH 7.4] with 0.6%, wt/vol, BSA without FCS) with or without (control) AMB/AMB-AGC. Then, fluorescein isothiocyanate-labeled human transferrin (FITC-hTfn) (60 μg/ml; Molecular Probes, Eugene, OR) binding was performed (60 min on ice). After washes with fresh medium, endocytosis was induced for 5 or 30 min at 37°C in medium supplemented with the indicated drugs. Postendocytic trafficking was stopped by washing the cells with cold phosphate-buffered saline (PBS) and then with 50 mM MES (morpholineethanesulfonic acid) buffer containing 200 mM NaCl (pH 5.0) to reduce membrane-bound FITC-hTfn (1 h, 4°C). The cells were fixed with 4% paraformaldehyde in PBS. The images were processed with ImageJ software.

Immunofluorescence microscopy. Following FITC-hTfn internalization, the cells were fixed and labeled with mouse anti-EEA1 antibodies (1:200) (BD Transduction Laboratories, Palo Alto, CA) and Cy5-conjugated goat anti-mouse IgG (1:200) (Jackson ImmunoResearch Laboratories, West Grove, PA). Images were captured with a Zeiss LSM710 confocal microscope equipped with a 63× oil-immersion objective. The colocalization of FITC-hTfn with early endosomal antigen 1 (EEA1) was quantified using Manders' coefficient in the JACoP macro in ImageJ (see http://rsbweb.nih.gov/ij/).

pH measurement of hTfn-positive endosomes. Endosomal pH was measured as described previously (35). Briefly, MDCK-PTR9 cells were grown in glass-bottom culture dishes (35-mm dish, 14-mm microwell) (MatTek Corp., Ashland, MA), and starvation, drug treatment, FITC-hTfn binding, and endocytosis were performed. Confocal images of live cells were taken using the FV-1000 confocal system (Olympus) based on an IX81 inverted microscope with a 60×/1.35 numerical aperture (NA) oil objective and Z-drive set to 1-μm increments between sections. The excitation wavelengths were 458 and 488 nm, and emission was collected with a 504-nm filter. Each dual-excitation image pair was imported into ImageJ 1.41n, where ~145 to 170 endosomes from 15 to 20 cells were classified as regions of interest. The pH was determined according to 488/458 emission ratios, and a pH calibration curve was prepared by incubating cells with internalized FITC-hTfn for 15 min with 10 mM MES or HEPES buffers containing 135 mM KCl, 5 mM dextrose, and 25 μM nigericin (Molecular Probes) at different pHs.

Statistics. Statistical significance was determined by Student's *t* test ($P \leq 0.05$).

RESULTS

AMB and AMB-AGC antifungal activity and effects on K^+ leakage. AMB-AGC retained its antifungal activity against *C. albicans* but at higher concentrations and slower kinetics than with free AMB (MICs of 0.5 versus 0.125 μg/ml) (Fig. 1A). The AMB and AMB-AGC concentrations that killed the fungi also induced K^+

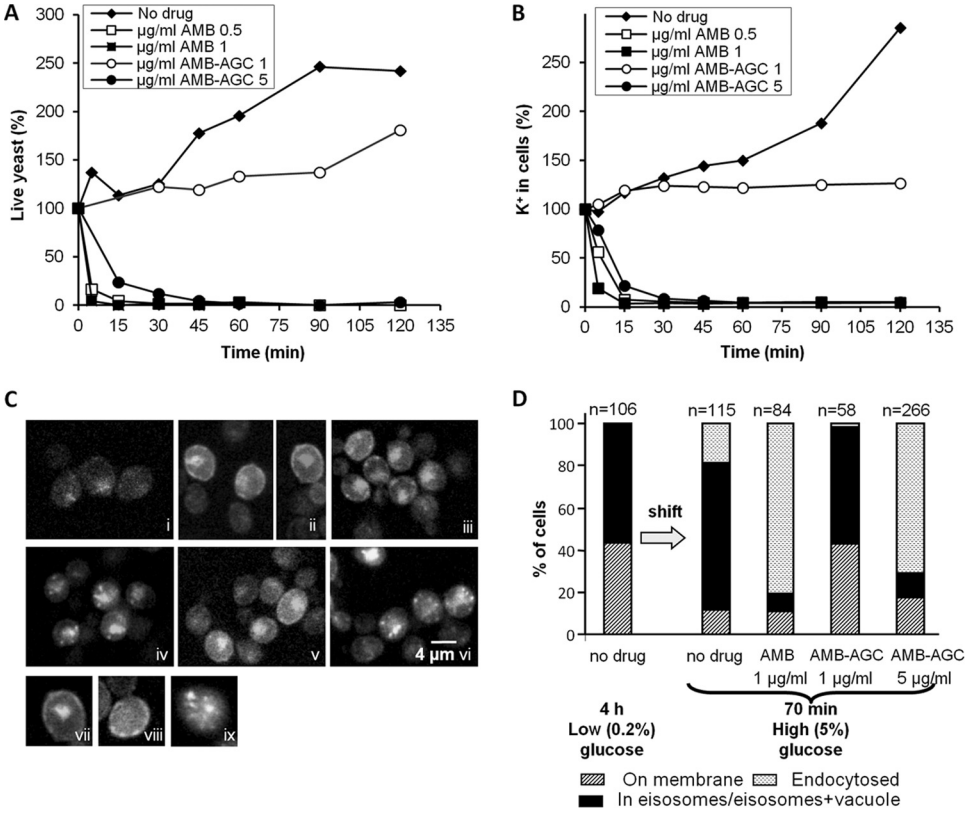

FIG 1 AMB and AMB-AGC killing kinetics, induction of K^+ leakage, and internalization of Hxt2-GFP from the PM to endosomal compartments in yeast. (A) *C. albicans* yeast cells were treated with AMB or AMB-AGC in YPD medium. Aliquots were collected at the indicated time points, and survival rates were determined (%CFU). Similar results were obtained when PBS was used instead of the YPD medium. (B) *C. albicans* yeast cells were treated with AMB or AMB-AGC. Aliquots were collected at the indicated time points and washed, and the internal K^+ concentration was determined by atomic absorption spectroscopy. (C) *S. cerevisiae* expressing the Hxt2-GFP construct were incubated in 5% glucose for 18 h (i) and then washed and transferred to 0.2% glucose for 4 h (ii). The yeast cells were then transferred again to 5% glucose for 70 min of no drug (control) (iii), 1 μg/ml AMB (iv), 1 μg/ml AMB-AGC (v), or 5 μg/ml AMB-AGC (vi). The yeast suspension was fixed with 4% paraformaldehyde (PFA) and visualized by fluorescence microscopy. Also shown are a cell with Hxt2-GFP in its PM and vacuole (vii), with Hxt2-GFP in the eisosomes (viii), and with Hxt2-GFP in the endosomal compartment (ix). (D) Quantification of the experiment shown in panel C. The cells were classified according to the localization of Hxt2-GFP (n = number of cells).

leakage from *C. albicans* cells (Fig. 1B), indicating AMB polar channel formation. Similar mortality results were obtained with the *Saccharomyces cerevisiae* CRY1 strain (S. Kagan and I. Polacheck, data not shown).

Effect of treatment with AMB and AMB-AGC on intracellular trafficking in *S. cerevisiae*. The effects of AMB and AMB-AGC on intracellular trafficking were studied in *S. cerevisiae* expressing the high-affinity glucose transporter fusion protein Hxt2-GFP (28, 57). Overnight incubation with a high glucose concentration (5%) resulted in a small amount of Hxt2-GFP being dispersed diffusely throughout the cells (Fig. 1Ci). Shifting the yeast to a low glucose concentration (0.2%) resulted in an increased amount of Hxt2-GFP, localized on the PM and in the vacuole (Fig. 1Cii). Shifting back to 5% glucose resulted in endocytosis of the Hxt2-GFP through the eisosomes (Fig. 1Ciii), as shown in previous studies (28, 57). Treatment with 1 μg/ml of AMB led to enhanced internalization of Hxt2-GFP into numerous small intracellular structures and not into a single vacuole (Fig. 1Civ). Treatment with a low concentration of AMB-AGC (1 μg/ml) resulted in an Hxt2-GFP localization pattern similar to that of the no-drug control (Fig. 1Cv), whereas treatment with 5 μg/ml AMB-AGC (Fig. 1Cvi) resulted in the same Hxt2-GFP localization pattern that was observed for 1 μg/ml AMB. The AMB-induced Hxt2-GFP internalization was not dependent on glucose concentration (S. Kagan and I. Polacheck, data not shown). Quantification of the results in Fig. 1C is presented in Fig. 1D. Taken together, the results in Fig. 1C and D indicate that treatment with AMB or AMB-AGC affects intracellular trafficking in yeast cells in a manner similar to that of free AMB in mammalian cells (10, 56).

Treatment with AMB or AMB-AGC increases vacuolar pH. We assumed that the effect of AMB treatment on intracellular trafficking is caused by the equalization of vacuolar and endosomal pHs with that of the cytosol, due to the internalization of the AMB polar channels. We examined vacuolar pH with BCECF-AM (Fig. 2), a fluorescent pH indicator that accumulates in the yeast vacuole (1, 13, 24, 40, 59). The treatment of *C. albicans* with AMB resulted in a sharp pH increase from 6.20 to between 6.64 and 6.75 (depending on AMB concentration), followed by a decrease to pH 6.0 to 6.3. These changes in pH were even seen at the low AMB concentration of 0.155 μg/ml (Fig. 2B). The effect of the treatment with AMB-AGC was similar to that of AMB but with slower kinetics (Fig. 2C).

AMB and AMB-AGC toxicities and membrane perforation in mammalian cells. The *in vitro* toxicities of both AMB and

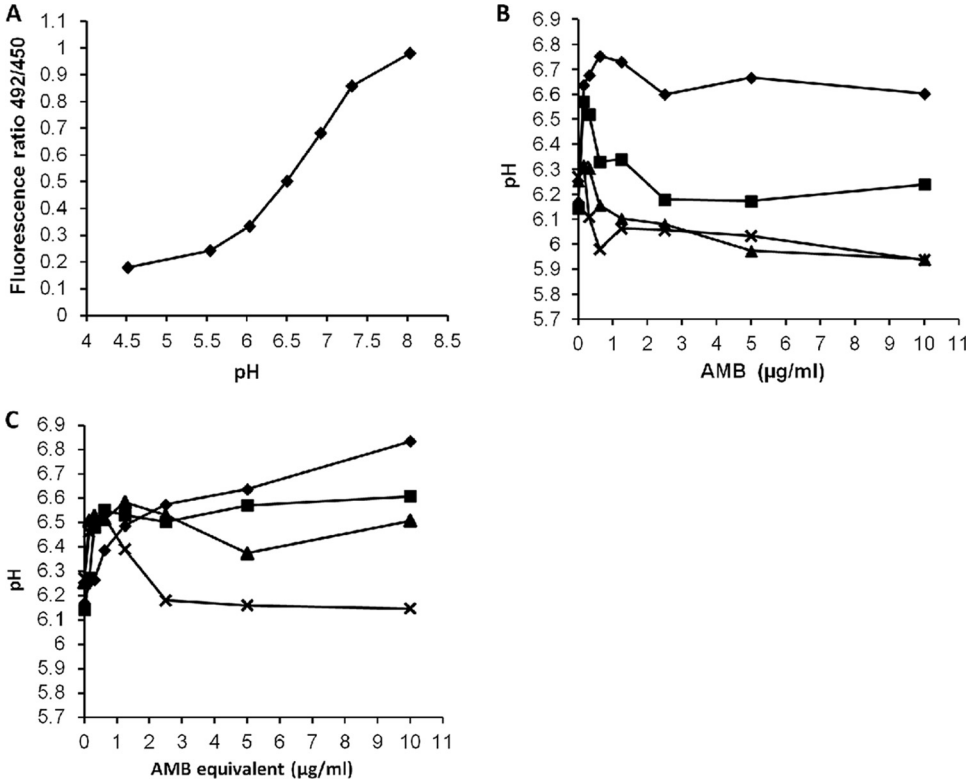

FIG 2 Increased vacuolar pH in *C. albicans* following treatment with AMB or AMB-AGC. (A) BCECF calibration curve. (B) BCECF-AM-labeled *C. albicans* treated with AMB. (C) BCECF-AM-labeled *C. albicans* treated with AMB-AGC. Fluorescence intensities were measured in panels B and C at different time points: ◆, 9 min; ■, 20 min; ▲, 35 min; **x**, 60 min. The pHs were calculated according to the calibration curve. For each examined concentration, statistical significance was found at maximal pH increase ($P < 0.05$).

AMB-AGC treatments were determined against two different epithelial kidney cell lines (Vero and MDCK-PTR9). Treatment with free AMB was highly toxic to both cell lines (4 μg/ml of AMB killed 30 to 35% of the cells), whereas the AMB-AGC was nontoxic, even at 100-fold the concentration of AMB (400 μg/ml) (Fig. 3A and B). Polar channel formation in the PM of mammalian cells was examined in two different model systems: hemolysis in sheep red blood cells (SRBCs) and K^+ leakage from Vero cells. Hemolysis was observed in SRBCs treated with 0.5 μg/ml free AMB, while even at the extremely high concentration of 10^4 μg/ml, AMB-AGC was nonhemolytic. K^+ leakage was observed from Vero cells after treatment with 2 and 4 μg/ml of free AMB, whereas no leakage was detected following treatment with AMB-AGC at the high concentration of 400 μg/ml (Fig. 3C). These results indicate that the conjugation of AMB with AG prevents PM perforation in mammalian cells.

Effects of AMB and AMB-AGC on receptor trafficking in MDCK cells. To investigate the influence of treatment with AMB and AMB-AGC on intracellular trafficking in MDCK cells, we studied their effects on the distribution of various receptors. Incubation of MDCK cells expressing the muscarinic receptor M1 fused to GFP (M1-GFP) with 40 μg/ml free AMB caused the redistribution of a significant fraction of the M1-GFP from the PM to endosomes, whereas the conjugation of AMB (even at 400 μg/ml) with AG prevented this redistribution (Fig. 4A). Similar results were obtained for the human chemokine receptor CXCR4 fused to GFP (see Fig. S1 in the supplemental material). We also investigated the effects of AMB and AMB-AGC on human transferrin receptor (hTfnR); this receptor is a classical nonraft protein that does not interact with caveolins (38, 52), in contrast to the M1 receptor and CXCR4, which physically interact with caveolins (46, 54, 55; Y. Altschuler, unpublished data). The effects of the drugs on hTfnR trafficking were studied by binding FITC-hTfn to the PM of MDCK-PTR9 cells treated with AMB or AMB-AGC, followed by short and long endocytosis (5 and 30 min, respectively). Neither AMB nor AMB-AGC prevented hTfn binding to the PM, indicating that they do not block hTfnR recycling from endosomes to the PM. In untreated cells, 5 min of endocytosis resulted in the localization of FITC-hTfn to punctate endosomes that resembled early endosomes (EEs) (see Discussion and reference 50) (see also Fig. S2A and B in the supplemental material). After 30 min of endocytosis, FITC-hTfn was localized to more reticulate perinuclear endosomal compartments resembling recycling endosomes (REs) (see Discussion and reference 50) (see also Fig. 4B and Fig. S2B). Treatment with AMB (10 μg/ml, 19 h) resulted in enlargement of some of the endosomes that were positive for FITC-hTfn after 5 min of endocytosis (EEs), particularly in the apical sections (see Fig. S2A and B); following 30 min of endocytosis, the FITC-hTfn-positive endosomes (REs) also became enlarged, and this enlargement was more significant than was the EE enlargement after the 5-min endocytosis (Fig. 4B; see also Fig. S2B). In addition, in AMB-treated cells, the REs were brighter and less reticular than in the control cells.

A longer incubation of the cells with AMB (24 h) resulted in

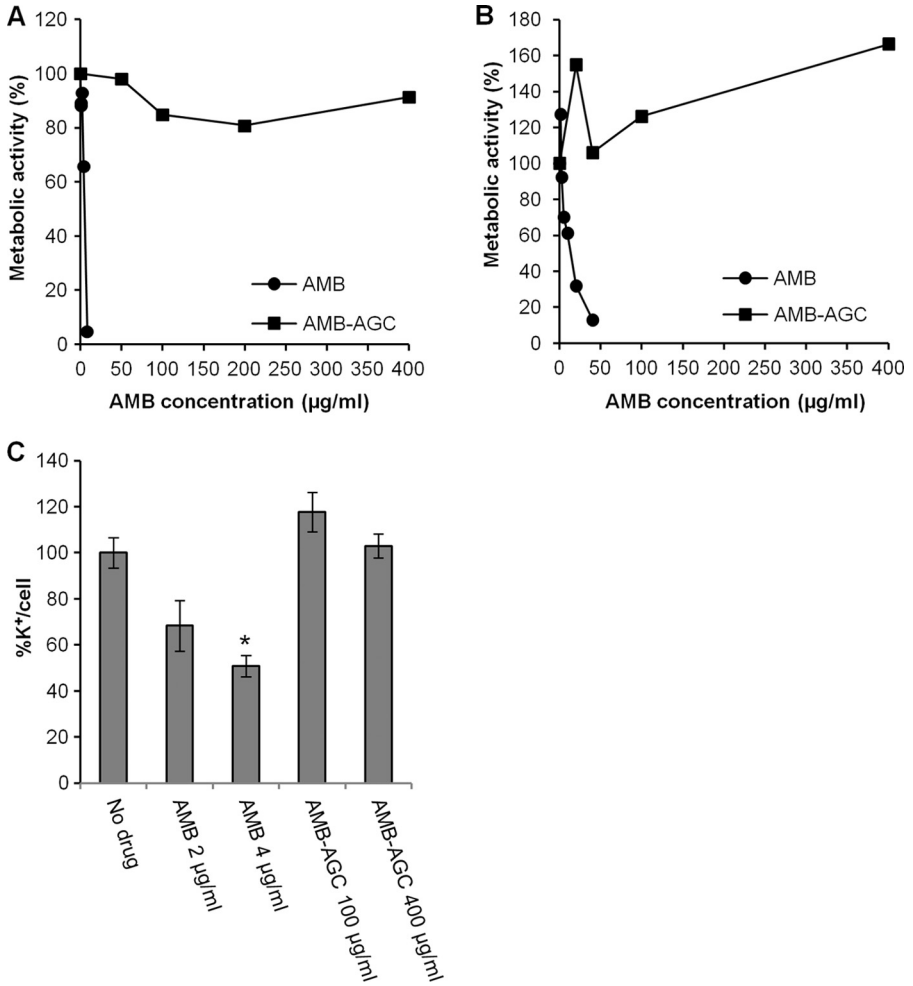

FIG 3 AMB-induced toxicity and K^+ leakage in kidney cell lines are abolished by the conjugation of AMB with AG. Vero cells were treated for 1 h (A) and MDCK-PTR9 cells for 19 h (B) with the specified concentrations of AMB or AMB-AGC, and the metabolic activity was measured by an XTT assay. (C) Vero cells were treated for 1 h with the indicated concentrations of AMB or AMB-AGC. The internal K^+ concentration was measured by atomic absorption spectrometry and normalized to the number of cells. The error bars show concentrations ± the SDs. One asterisk represents a *P* value of 0.0032 compared to the value for the no-drug control.

massive tubulation of the FITC-hTfn-containing REs (Fig. 4B; see also Fig. S2B in the supplemental material), which was not observed in the EEs (see Fig. S2A and B). No significant changes in the endosomal compartments were observed after treatment with 400 μg/ml AMB-AGC (19 h or 24 h) (Fig. 4B; see also Fig. S2A and B). Early endosomal antigen 1 (EEA1), a classical EE marker, was used to investigate the effects of the drugs on hTfnR transport from the EEs to the REs. Following the internalization of FITC-hTfn, the fixed cells were stained with anti-EEA1 antibody. Figure S2B shows that the EEA1 partially colocalized with the 5-min-internalized FITC-hTfn and was frequently localized in adjacent domains of the same endosome. The enlargement of some of the EEA1-positive endosomes could be seen after AMB treatment, and these endosomes were separate from the tubulated REs. Quantification of the FITC-hTfn that colocalized with EEA1 (Fig. 4C) showed that 19 h of treatment with free AMB did not affect the colocalization of 5-min-internalized FITC-hTfn with EEA1. However, this treatment increased the colocalization of 30-min-internalized FITC-hTfn with EEA1, indicating partial inhibition of the exit of FITC-hTfn from the EE compartment. This effect of AMB was prevented by its conjugation with AG. A long incubation with the drugs, as in the experiments described above, was performed to detect the possible effects of AMB-AGC, but the enlargement of REs could be seen even after 2 h of treatment with 10 to 20 μg/ml free AMB (see Fig. S2C). Thus, AMB did not block hTfnR trafficking from the EEs to the REs, but it partially inhibited this step and changed the morphology of EEs and REs. This effect was abolished by the conjugation of AMB with AG.

Effects of AMB and AMB-AGC on endosomal pH. The effects of the drugs on endosomal pH were measured by the fluorescence intensity of endocytosed FITC-hTfn in MDCK cells; the fluorescence intensity ratios following excitation at 488 and 458 nm were proportional to the increases in pH (Fig. 5A). A chart showing the mean endosomal pHs in the variously treated cells is presented in Fig. 5B. The pH in untreated cells was 5.73, similar to the known pH of REs in MDCK-PTR9 cells (58). Treatment with AMB, but not AMB-AGC, caused endosomal alkalization that increased the pH to 7.2, which is equivalent to the cytosolic pH. Thus, in contrast to free AMB, the conjugated AMB maintained the endosomal pH gradient that is required for normal membrane trafficking.

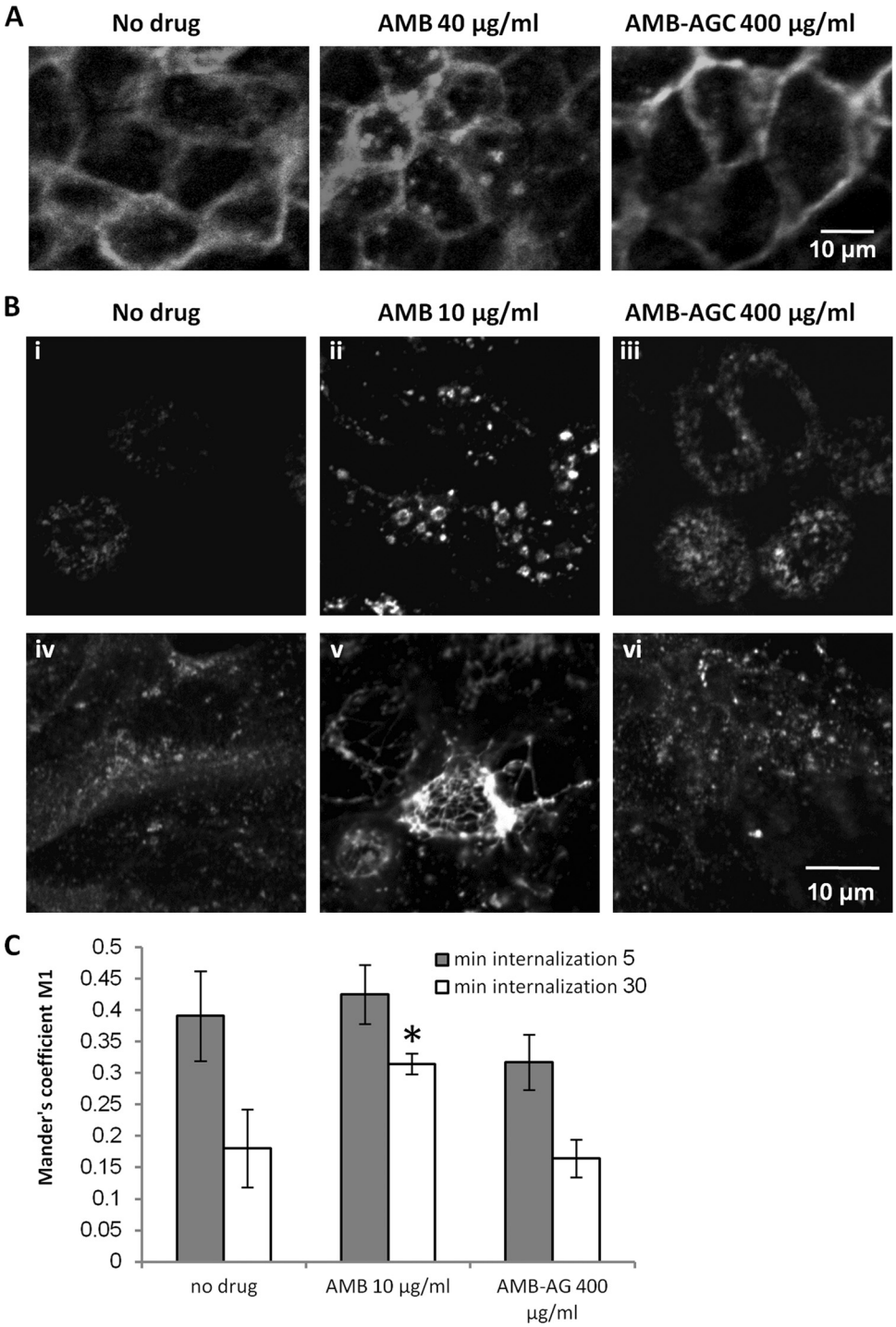

FIG 4 AMB, but not AMB-AGC, modulates the distribution of receptors in MDCK cells. (A) MDCK cells stably expressing M1-GFP were grown on glass coverslips and treated for 1 h with no drug (control), 40 μg/ml AMB, or 400 μg/ml AMB-AGC. The cells were visualized by fluorescence microscopy after fixation. (B) MDCK-PTR9 cells grown on glass coverslips in MEM/BSA medium were treated for 19 h (i to iii) or 24 h (iv to vi) with AMB (10 μg/ml), AMB-AGC (400 μg/ml), or no drug (control) and then incubated with 60 mg/ml of FITC-hTfn for 60 min on ice to induce binding. After intensive washing, the cells were transferred to fresh medium and incubated at 37°C for 30 min to enable endocytosis. The cells were then washed with acidic buffer to strip membrane-attached FITC-hTfn from the membrane, fixed, and visualized by confocal microscopy. (C) After FITC-hTfn internalization and fixation (19 h treatment), the cells were labeled with mouse anti-EEA1 and then with Cy5-conjugated goat anti-mouse IgG. The samples were documented by confocal microscopy, and quantification of FITC-hTfn colocalization with EEA1 was performed. The Manders' M1 coefficients are presented. Colocalization analyses were performed for at least 20 cells in at least four different microscopic fields. The error bars represent Manders' M1 coefficients ± the SDs. One asterisk represents a *P* value of 0.00197 compared to the value for the no-drug control. Gray and white columns represent internalization for 5 and 30 min, respectively.

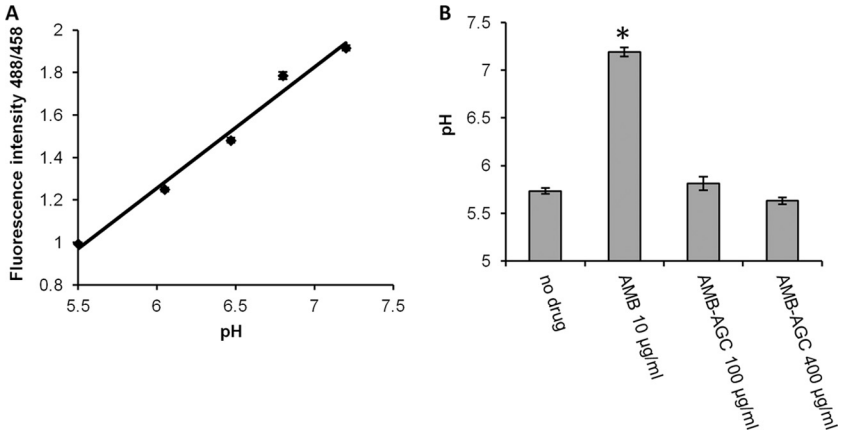

FIG 5 The AMB-induced increase in endosomal pH in kidney cells is abolished by conjugation with AG. (A) Calibration curve of FITC-hTfn fluorescence intensity in MDCK-PTR9 cell endosomes as a function of pH. (B) MDCK-PTR9 cells were treated with AMB or AMB-AGC for 18 h, followed by 60 min of incubation on ice with 60 μg/ml FITC-hTfn to induce binding. After intensive washing, the cells were transferred to fresh medium and incubated at 37°C for 30 min to enable endocytosis. The samples were documented by confocal microscopy, and the pH was calculated as described in Materials and Methods. The columns show the average pHs (± the standard errors of the mean) of 145 to 170 endosomes in at least 16 different cells. One asterisk represents a *P* value of <0.0001 compared to the value for the no-drug control.

DISCUSSION

We found that in both mammalian and fungal cells, free AMB perforates the PM, modulates intracellular trafficking, and abolishes the pH gradient between the endosomes/vacuole and the cytosol. The conjugation of AMB with AG neutralized these effects in mammalian but not in fungal cells. To the best of our knowledge, this is the first demonstration of AMB treatment causing endosomal alkalization in mammalian cells and intracellular trafficking perturbations in fungal cells.

AMB modulation of intracellular trafficking has been shown in mammalian cells (10, 56). We found that AMB treatment modulates the trafficking of three receptors: CXCR4 and the M1 receptor, which interact with caveolins (51; Y. Altschuler, unpublished data), and hTfnR, a classical nonraft receptor that does not interact with caveolins (38, 52). Despite its interaction with caveolins, the M1 receptor is not localized in the caveolae (51). Thus, the effects of AMB on intracellular trafficking are not restricted to proteins localized in the caveolae or to those associated with caveolins. AMB treatment caused a dramatic redistribution of the M1 receptor and CXCR4 from the PM to the endosomes, indicating significant inhibition of the recycling of these receptors from the endosomes to the PM. This AMB-induced relocalization is similar to that shown for caveolins 1 and 3 (10) and is consistent with the finding that recycling of the M1 receptor and CXCR4 is inhibited by association with caveolins (51; Y. Altschuler, unpublished data).

Sheff et al. (50) described the hTfnR trafficking pathway as follows: endocytosed hTfn-hTfnR arrives at the punctate peripheral endosomal compartment known as EE. From there, a fraction of the hTfn-hTfnR is recycled directly to the PM via a shorter route, while another fraction is recycled to the PM via a longer route, through a perinuclear endosomal compartment designated RE. Additional studies showed that after 2 to 5 min of endocytosis, most of the hTfn is localized in the EEs, whereas after 20 to 30 min of endocytosis, it is mostly localized in the REs (9, 29, 50). We found that treatment with AMB does not prevent hTfn binding to the PM, indicating that it does not block the recycling of hTfnR from the endosomes. In addition, AMB did not block hTfnR trafficking from the EEs to the REs, but it partially inhibited this step and also changed the morphology of the EEs and REs. These findings indicate that hTfnR trafficking is moderately affected by AMB treatment. In addition, we found that AMB treatment increases pH in the REs, causing its equalization with cytosolic pH.

So far, the mode of action of AMB against fungi has been only partially understood; in particular, the role of vacuolar pH modulation has been neglected (to the best of our knowledge, there has been only one study of its role [59]). We found that in fungi, AMB treatment perturbs intracellular trafficking and induces an increase in vacuolar pH. The vacuolar pH increase in *C. albicans* is followed by a pH decrease, which can be explained by cytosol acidification as described by Rabaste et al. (44). Thus, we believe that pH modulation underlies AMB's mode of action against fungi.

Taken together, these results indicate that in both fungal and mammalian cells, in addition to PM perforation, AMB treatment modulates intracellular membrane trafficking as part of its mechanism of activity, and it also abolishes the pH gradient between the cytosol and acidic compartments, such as endosomes and vacuoles. The finding that AMB modulates vacuolar pH at a low concentration (0.155 μg/ml) supports the hypothesis that this modulation is caused by a perforation of the vacuolar membrane due to endocytosis of the AMB polar channels. As a result of channel endocytosis, H^+ ions leak out of the endosomes/vacuoles to the cytosol, resulting in abolishment of the pH gradient, which may lead to the inhibition or blockage of some trafficking pathways (Fig. 6).

Our results in mammalian cells regarding hTfnR trafficking and endosomal alkalization (Fig. 4B and C and 5; see also Fig. S2 in the supplemental material), combined with published evidence that hTfnR recycling is retarded but not abolished by endosomal alkalization (27, 42, 43), support the hypothesis that AMB interferes with intracellular trafficking through endosomal alkalization (56). However, the current study does not provide sufficient evidence to prove a causative connection between endosomal/

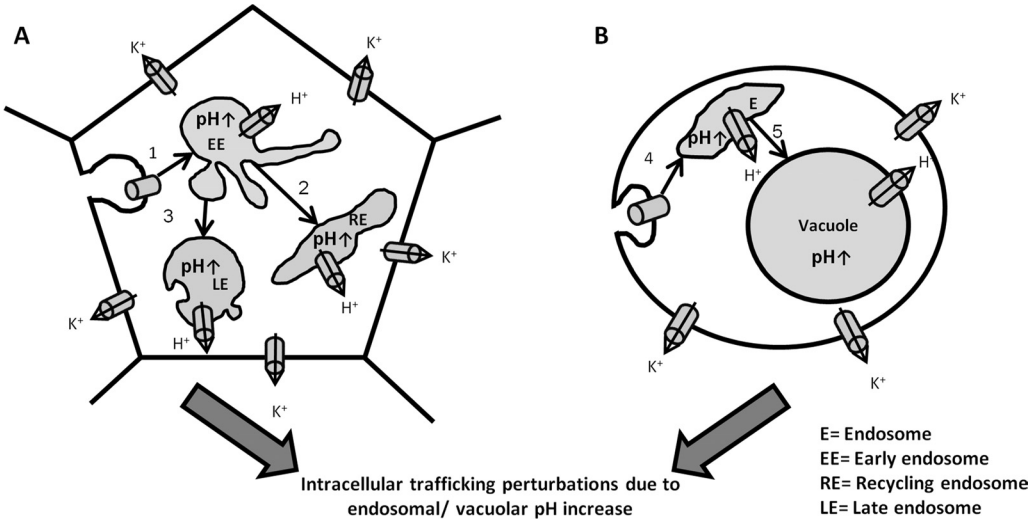

FIG 6 A proposed model for AMB activity in mammalian and fungal cells. AMB forms polar channels in mammalian PM (A) and fungal PM (B), which results in ion and metabolite leakage out of the cells. In addition, the AMB channels endocytose into endosomes (steps 1 and 4). In fungal cells, they arrive at the vacuole by postendocytic trafficking (step 5), while in mammalian cells they are transferred from early endosomes to the recycling endosomes and late endosomes (steps 2 and 3). The AMB channels in endosomes and vacuoles allow H^+ leakage to the cytosol, leading to an endosomal/vacuolar pH increase, which in turn perturbs the trafficking steps.

vacuolar alkalization and perturbations in intracellular trafficking during AMB treatment; the possibility that the trafficking perturbations are an additional separate mechanism of AMB activity cannot be ruled out. Further research is required to distinguish between these two possibilities. This might include an investigation of the effects of alkalizing agents (bafilomycin A_1 or NH_4Cl [21, 23, 27, 43]) on receptor trafficking in MDCK cells and a study of the effect of AMB on Hxt2-GFP trafficking in *S. cerevisiae* strains harboring mutations in the genes involved in vacuolar pH regulation, such as *Drs2* and *Erg* (8).

We previously showed in a mouse model that the conjugation of AMB with AG causes a dramatic reduction in the toxicity of AMB but does not change its therapeutic efficacy (18). Similar data were obtained in the current *in vitro* study. To explain the different effects of AMB-AGC in mammalian and fungal cells, we examined its effects on membrane perforation, postendocytic trafficking, and intraendosomal/vacuolar pH in these cells.

The conjugation of AMB with AG abolished the AMB-induced PM perforation in mammalian cells, as shown in two different models: K^+ leakage from Vero cells and hemolysis of SRBCs. In addition, conjugation abolished all AMB-induced effects on postendocytic trafficking and prevented the endosomal pH increase in mammalian cells (MDCK). In fungal cells (*C. albicans* and *S. cerevisiae*), the conjugation of AMB with AG did not eliminate its antifungal activities as expressed by PM perforation, the blockage of intracellular trafficking (demonstrated by Hxt2-GFP localization), the modulation of vacuolar pH, and cell killing.

In summary, the reduced toxicity of AMB-AGC in mammalian cells can be explained by its failure to form polar channels in the PM, even at high concentrations, resulting in the absence of perforated endosomes and retention of the endosomal pH gradient. We assume that the modified traffic is a result of endosomal/vacuolar pH alkalization and that the lack of an effect of the AMB-AGC on trafficking is due to preservation of the pH gradient.

We hypothesize that the different effects of AMB-AGC in mammalian and fungal cells can be explained by the hindrance of self-association of the AMB molecule by the AG conjugate scaffold. Previous studies have shown that the self-association of AMB molecules in medium is required to form AMB channels in cholesterol-containing membranes (mammalian), whereas in ergosterol-containing membranes (fungi), monomeric AMB molecules are sufficient to form polar channels (6, 25, 26, 31, 32). Therefore, while free AMB can form polar channels in both mammalian and fungal membranes, conjugated AMB can only perforate fungal membranes. We think that this is a reasonable explanation for the specific neutralization of AMB toxicity in mammalian cells.

REFERENCES

1. **Ali R, Brett CL, Mukherjee S, Rao R.** 2004. Inhibition of sodium/proton exchange by a Rab-GTPase-activating protein regulates endosomal traffic in yeast. J. Biol. Chem. **279**:4498–4506.
2. **Altschuler Y, et al.** 1999. ADP-ribosylation factor 6 and endocytosis at the apical surface of Madin-Darby canine kidney cells. J. Cell Biol. **147**:7–12.
3. **Arnold TM, Dotson E, Sarosi GA, Hage CA.** 2010. Traditional and emerging antifungal therapies. Proc. Am. Thorac. Soc. **7**:222–228.
4. **Baginski M, Resat H, Borowski E.** 2002. Comparative molecular dynamics simulations of amphotericin B-cholesterol/ergosterol membrane channels. Biochim. Biophys. Acta **1567**:63–78.
5. **Bolard J.** 1986. How do the polyene macrolide antibiotics affect the cellular membrane properties? Biochim. Biophys. Acta **864**:257–304.
6. **Bolard J, Legrand P, Heitz F, Cybulska B.** 1991. One-sided action of amphotericin B on cholesterol-containing membranes is determined by its self-association in the medium. Biochemistry **30**:5707–5715.
7. **Brajtburg J, Bolard J.** 1996. Carrier effects on biological activity of amphotericin B. Clin. Microbiol. Rev. **9**:512–531.
8. **Brett CL, et al.** 2011. Genome-wide analysis reveals the vacuolar pH-stat of *Saccharomyces cerevisiae*. PLoS One **6**:e17619. doi:10.1371/journal.pone.0017619.
9. **Brown PS, et al.** 2000. Definition of distinct compartments in polarized Madin-Darby canine kidney (MDCK) cells for membrane-volume sorting, polarized sorting and apical recycling. Traffic **1**:124–140.
10. **Carozzi AJ, Ikonen E, Lindsay MR, Parton RG.** 2000. Role of cholesterol

in developing T-tubules: analogous mechanisms for T-tubule and caveolae biogenesis. Traffic **1**:326–341.
11. **Clinical and Laboratory Standards Institute.** 2008. Reference method for broth dilution antifungal susceptibility testing for yeasts. Approved standard, third edition. M27-A3, vol 28. Clinical and Laboratory Standards Institute, Wayne, PA.
12. **Czub J, Baginski M.** 2006. Modulation of amphotericin B membrane interaction by cholesterol and ergosterol—a molecular dynamics study. J. Phys. Chem. B **110**:16743–16753.
13. **Davies JM, Brownlee C, Jennings DH.** 1990. Measurement of intracellular pH in fungal hyphae using BCECF and digital imaging microscopy: evidence for a primary proton pump in the plasmalemma of a marine fungus. J. Cell Sci. **96**:731–736.
14. **Deray G.** 2002. Amphotericin B nephrotoxicity. J. Antimicrob. Chemother. **49**(Suppl 1):37–41.
15. **Desbuquois B, et al.** 1992. Role of acidic subcellular compartments in the degradation of internalized insulin and in the recycling of the internalized insulin receptor in liver cells: in vivo and in vitro studies. Diabete Metab. **18**:104–112.
16. **Dupont B.** 2002. Overview of the lipid formulations of amphotericin B. J. Antimicrob. Chemother. **49**(Suppl 1):31–36.
17. **Ehrenfreund-Kleinman T, et al.** 2002. Synthesis and characterization of novel water soluble amphotericin B-arabinogalactan conjugates. Biomaterials **23**:1327–1335.
18. **Falk R, Domb AJ, Polacheck I.** 1999. A novel injectable water-soluble amphotericin B-arabinogalactan conjugate. Antimicrob. Agents Chemother. **43**:1975–1981.
19. **Falk R, et al.** 2005. Induction of interleukin-1beta, tumour necrosis factor-alpha and apoptosis in mouse organs by amphotericin B is neutralized by conjugation with arabinogalactan. J. Antimicrob. Chemother. **55**:713–720.
20. **Fanos V, Cataldi L.** 2000. Amphotericin B-induced nephrotoxicity: a review. J. Chemother. **12**:463–470.
21. **Gekle M, Mildenberger S, Freudinger R, Silbernagl S.** 1995. Endosomal alkalinization reduces Jmax and Km of albumin receptor-mediated endocytosis in OK cells. Am. J. Physiol. **268**:F899–F906.
22. **Hartsel SC, Hatch C, Ayenew W.** 1993. How does amphotericin B work? Studies on model membrane systems. J. Liposome Res. **3**:377–408.
23. **Heinzelmann M, Platz A, Flodgaard H, Polk HC, Jr, Miller FN.** 1999. Endocytosis of heparin-binding protein (CAP37) is essential for the enhancement of lipopolysaccharide-induced TNF-alpha production in human monocytes. J. Immunol. **162**:4240–4245.
24. **Hernlem BJ, Srienc F.** 1989. Intracellular pH in single *Saccharomyces cerevisiae* cells. Biotechnol. Tech. **3**:79–84.
25. **Hirano M, Takeuchi Y, Matsumori N, Murata M, Ide T.** 2011. Channels formed by amphotericin B covalent dimers exhibit rectification. J. Membr. Biol. **240**:159–164.
26. **Huang W, et al.** 2002. Ion channel behavior of amphotericin B in sterol-free and cholesterol- or ergosterol-containing supported phosphatidylcholine bilayer model membranes investigated by electrochemistry and spectroscopy. Biophys. J. **83**:3245–3255.
27. **Johnson LS, Dunn KW, Pytowski B, McGraw TE.** 1993. Endosome acidification and receptor trafficking: bafilomycin A1 slows receptor externalization by a mechanism involving the receptor's internalization motif. Mol. Biol. Cell **4**:1251–1266.
28. **Kruckeberg AL, Ye L, Berden JA, van Dam K.** 1999. Functional expression, quantification and cellular localization of the Hxt2 hexose transporter of *Saccharomyces cerevisiae* tagged with the green fluorescent protein. Biochem. J. **339**(Pt 2):299–307.
29. **Lakadamyali M, Rust MJ, Zhuang X.** 2006. Ligands for clathrin-mediated endocytosis are differentially sorted into distinct populations of early endosomes. Cell **124**:997–1009.
30. **Laniado-Laborin R, Cabrales-Vargas MN.** 2009. Amphotericin B: side effects and toxicity. Rev. Iberoam Micol. **26**:223–227.
31. **Legrand P, Romero EA, Cohen BE, Bolard J.** 1992. Effects of aggregation and solvent on the toxicity of amphotericin B to human erythrocytes. Antimicrob. Agents Chemother. **36**:2518–2522.
32. **Matsumori N, Yamaji N, Matsuoka S, Oishi T, Murata M.** 2002. Amphotericin B covalent dimers forming sterol-dependent ion-permeable membrane channels. J. Am. Chem. Soc. **124**:4180–4181.
33. **Mellman I, Fuchs R, Helenius A.** 1986. Acidification of the endocytic and exocytic pathways. Annu. Rev. Biochem. **55**:663–700.
34. **Miceli MH, Diaz JA, Lee SA.** 2011. Emerging opportunistic yeast infections. Lancet Infect. Dis. **11**:142–151.
35. **Mitchell J, et al.** 2008. An expanded biological repertoire for Ins(3,4,5,6)P4 through its modulation of ClC-3 function. Curr. Biol. **18**:1600–1605.
36. **Moen MD, Lyseng-Williamson KA, Scott LJ.** 2009. Liposomal amphotericin B: a review of its use as empirical therapy in febrile neutropenia and in the treatment of invasive fungal infections. Drugs **69**:361–392.
37. **Nishi KK, et al.** 2007. Amphotericin B-gum Arabic conjugates: synthesis, toxicity, bioavailability, and activities against Leishmania and fungi. Pharm. Res. **24**:971–980.
38. **Nothdurfter C, Rammes G, Rein T, Rupprecht R.** 2007. Pitfalls in isolating lipid rafts. Nat. Rev. Neurosci. **8**:567.
39. **Odds FC, Brown AJ, Gow NA.** 2003. Antifungal agents: mechanisms of action. Trends Microbiol. **11**:272–279.
40. **Polacheck I, Antman A, Barth I, Sagi E, Giloh H.** 1995. Adherence of *Candida albicans* to epithelial cells: studies using fluorescently labelled yeasts and flow cytometry. Microbiology **141**:1523–1533.
41. **Polacheck I, et al.** 1991. Mode of action of the antimycotic agent G2 isolated from alfalfa roots. Zentralbl. Bakteriol. **275**:504–512.
42. **Presley JF, et al.** 1993. The End2 mutation in CHO cells slows the exit of transferrin receptors from the recycling compartment but bulk membrane recycling is unaffected. J. Cell Biol. **122**:1231–1241.
43. **Presley JF, Mayor S, McGraw TE, Dunn KW, Maxfield FR.** 1997. Bafilomycin A1 treatment retards transferrin receptor recycling more than bulk membrane recycling. J. Biol. Chem. **272**:13929–13936.
44. **Rabaste F, Sancelme M, Delort AM.** 1995. Modifications of pH and K+ gradients in *Candida albicans* blastospores induced by amphotericin B. A 31P NMR and K+ atomic absorption study. Biochim. Biophys. Acta **1268**:50–58.
45. **Resat H, Baginski M.** 2002. Ion passage pathways and thermodynamics of the amphotericin B membrane channel. Eur. Biophys. J. **31**:294–305.
46. **Sbaa E, et al.** 2006. Caveolin plays a central role in endothelial progenitor cell mobilization and homing in SDF-1-driven postischemic vasculogenesis. Circ. Res. **98**:1219–1227.
47. **Sedlak M, Drabina P, Bilkova E, Simunek P, Buchta V.** 2008. New targeting system for antimycotic drugs: beta-glucosidase sensitive amphotericin B-star poly(ethylene glycol) conjugate. Bioorg. Med. Chem. Lett. **18**:2952–2956.
48. **Sedlak M, Pravda M, Kubicova L, Mikulcikova P, Ventura K.** 2007. Synthesis and characterisation of a new pH-sensitive amphotericin B–poly(ethylene glycol)-*b*-poly(L-lysine) conjugate. Bioorg. Med. Chem. Lett. **17**:2554–2557.
49. **Sedlak M, et al.** 2007. Synthesis of pH-sensitive amphotericin B-poly(ethylene glycol) conjugates and study of their controlled release in vitro. Bioorg. Med. Chem. **15**:4069–4076.
50. **Sheff DR, Daro EA, Hull M, Mellman I.** 1999. The receptor recycling pathway contains two distinct populations of early endosomes with different sorting functions. J. Cell Biol. **145**:123–139.
51. **Shmuel M, Nodel-Berner E, Hyman T, Rouvinski A, Altschuler Y.** 2007. Caveolin 2 regulates endocytosis and trafficking of the M1 muscarinic receptor in MDCK epithelial cells. Mol. Biol. Cell **18**:1570–1585.
52. **Souto RP, et al.** 2003. Immunopurification and characterization of rat adipocyte caveolae suggest their dissociation from insulin signaling. J. Biol. Chem. **278**:18321–18329.
53. **Thompson GR, III, Cadena J, Patterson TF.** 2009. Overview of antifungal agents. Clin. Chest Med. **30**:203–215.
54. **van Buul JD, et al.** 2003. Leukocyte-endothelium interaction promotes SDF-1-dependent polarization of CXCR4. J. Biol. Chem. **278**:30302–30310.
55. **Venkatesan S, Rose JJ, Lodge R, Murphy PM, Foley JF.** 2003. Distinct mechanisms of agonist-induced endocytosis for human chemokine receptors CCR5 and CXCR4. Mol. Biol. Cell **14**:3305–3324.
56. **Vertut-Doi A, Ohnishi SI, Bolard J.** 1994. The endocytic process in CHO cells, a toxic pathway of the polyene antibiotic amphotericin B. Antimicrob. Agents Chemother. **38**:2373–2379.
57. **Walther TC, et al.** 2006. Eisosomes mark static sites of endocytosis. Nature **439**:998–1003.
58. **Wang E, et al.** 2000. Apical and basolateral endocytic pathways of MDCK cells meet in acidic common endosomes distinct from a nearly-neutral apical recycling endosome. Traffic **1**:480–493.
59. **Ziegelbauer K, Grusdat G, Schade A, Paffhausen W.** 1999. High throughput assay to detect compounds that enhance the proton permeability of *Candida albicans* membranes. Biosci. Biotechnol. Biochem. **63**:1246–1252.